Journal of the Korean Physical Society, Vol. 22, No. 3, September, 1989

Gain Calculation for a Tapered Free Electron Laser with an Axial Guide Field

Tae Hun Chung and Hyung Jin Kim
Department of Physics, Dong-A University, Saha-Gu, Pusan 604-714

(Received 23 March 1989)

A tapered free-electron laser with an axial guide field is analyzed using the linear fluid theory. The equation of motion and the constant of motion for an electron in this device are determined and the gain coefficient is formulated. The dependence of gain on the normalized vector potential, the degree of taper in the wiggler period, the strength of the wiggler field and the guide field, and the wiggler period are investigated.

I. INTRODUCTION

In recent years, extensive efforts have been devoted to finding a new mechanism for the production of electromagnetic radiation by a relativistic electron beam (REB) interacting with a spatially modulated static magnetic field. The development of a laser in which the active medium is a relativistic stream of free electrons has recently evoked much interest.

Free-electron lasers (FEL's) based on backscattering from REB have demonstrated a unique potential for becoming a new type of coherent radiation source. The coherence arises from the trapping and bunching of the electron beam in the ponderomotive potential well generated by the stimulated radiation and the static magnetic field (wiggler). The wiggler acts as a pump wave for a three wave interaction which will be described in Section II. The wiggler serves to impart a sufficient transverse oscillating motion to the beam electron to interact with the radiation that is amplified. The wiggler field is commonly generated by a periodical helical winding around the drift tube, usually distinct from the coils that provide the strong axial guide field.

An electron in a wiggler field is commonly thought to execute a simple helical motion corresponding to the periodicity of the imposed field. The output wavelength is determined by a double Doppler shift of the wiggler magnet period. The output power of the laser is proportional to the number of electrons which can be trapped in the ponderomotive well. In the Stanford experiment[1], Deacon et al. were able to operate an FEL above threshold at a wavelength of 3.4 μm, while high power microwaves have been detected in the Columbia experiment[2]. Other microwave generation processes analogous to these experiments have been explored at the Naval Research Laboratory[3] and Cornell University[4].

The ratio of the Debye length in the electron beam to the scattered wavelength has also proven to be an important beam frame parameter. When this ratio is large, Stimulated Compton Scattering (SCS) may occur. When it is small, however, the stimulated scattering process changes in character and can best be described as Stimulated Raman Scattering (SRS). In most cases the SCS has a gain which is too small to be useful for practical purpose. In order for valid application of the fluid theory, the condition $k\lambda_D \ll 1$, should be fulfilled, that is, the system should be in the Raman regime [5]. This condition requires a cold beam (small Δp), an intense electron beam (I<1 KA) and a relatively low electron energy (γ_o<10).[6]

These experimental conditions, especially the high beam current, can better be met in the presence of an axial guide field in addition to the helical wiggler conventionally used in FEL experiments. The presence of an axial guide magnetic field serves to collimate the high current electron beam in the interaction region.

The tapered wiggler[7-13] free-electron laser is a candidate as a high efficiency, tunable source of coherent radiation. The tapered version differs from the first FEL, which has demonstrated at Stanford University, in that the resonant electron energy of the wiggler magnet varies along the wiggler length so that the electron-photon resonant interaction is maintained as the electron decelerates. This resonant energy change results from variation of the wiggler magnetic field wavelength or amplitude as a function of axial position. Electrons trapped in the ponderomotive potential well decelerate in accordance with the resonant energy change, or the taper of the wiggler. This technique leads to significantly larger electron kinetic energy extraction than is possible with a constant parameter wiggler.

The first results were reported for an FEL experiment that utilized a tapered wiggler with a 2.25% magnetic field taper for efficiency enhancement by H. Boehmer et al.[14] The reported results of the Los Alamos FEL experiment show that the efficiency for converting electron beam energy to laser light at 10 μm was 1.3 percent for a tapered wiggler.[15] J. M. Slater et al. reported that the highest net energy extraction is 2.5% but with less than optimal trapping over the length of the wiggler with 9% taper. Five months later they again used the 9% tapered wiggler and observed a 4% net extraction with 50% electron trapping.[16] This suggests the possibility that the percentage decrease in the wiggler period can range from 0% up to 25%.[17] In addition, the tapered-wiggler experimental at Lawrence Livemore National Laboratory reported an efficiency of 35%.[18]

This paper formulates the gain coefficient phenomenologically. Then we investigate the dependence of gain coefficient on the normalized vector potential (a_ω), on the degree of taper in the wiggler period, and on the strength of the wiggler field and the axial guide field. We also examine the dependence of the gain coefficient on the wiggler period.

Section II gives the equation of motion of an electron in a tapered FEL and the gain formula, which is our major goal.

Section III shows the results of the gain calculation for various parameters. In Section IV, the conclusions are summarized.

II. THEORY

A homogeneous axial guide field is added to a right-handed helical magnetic wiggler

$$\boldsymbol{B}_o=\boldsymbol{B}_{oz}+\delta B(\hat{e}_x\cos k_o z+\hat{e}_y\sin k_o z) \tag{1}$$

where B_{oz} and δB measure the strength of the guide magnetic field and the wiggler magnetic field, respectively, and k_o is the wavenumber of the wiggler field.

The zeor-order response of the electron-beam through the helical field is[19]

$$\boldsymbol{v}_o=v_{oz}\hat{e}_z+\frac{\omega_{ce}k_o}{\gamma_o\kappa^2}(\hat{e}_x\cos k_o z+\hat{e}_y\sin k_o z) \tag{2}$$

where $\omega_{ce}=\dfrac{e\delta B}{mc}$ is the electron cyclotron frequency in the helical wiggler field, γ_o is the relativistic factor, and $\kappa^2=-k_o^2+\dfrac{k_o\Omega_{ce}}{\gamma_o v_{oz}}$ where Ω_{ce} is the electron cyclotron frequency in the axial homogeneous magnetic field.

This device involves a three-wave parameteric process in which a scattered EM wave grows as a result of the interaction between a pump wave (a periodic magnetostatic ripple in the laboratory frame) and a negative energy beam collective mode. The term which drives the scattered wave is the nonlinear current, and the idler (plasma wave) is again excited through the ponderomotive interaction. This subsequent excitation of the idler amplifies the scattered wave through coupling with the pump wave, and thus the stimulated scattering process occurs.

The EM wave to be amplified is chosen to be right-handed polarized and is given by

$$\begin{aligned}\boldsymbol{E}&=E_l[\hat{e}_x\cos(kz-\omega t+\theta)-\hat{e}_y\sin(kz-\omega t+\theta)],\\ \boldsymbol{B}&=B_l[\hat{e}_x\sin(kz-\omega t+\theta)+\hat{e}_y\cos(kz-\omega t+\theta)],\end{aligned} \tag{3}$$

where θ is the phase angle between the electron and the EM wave.

Due to the presence of the EM wave, the linear response of the electron beam to the applied field is

$$\begin{aligned}v=&[1-\frac{1}{\gamma_o^2}]^{\frac{1}{2}}c\hat{e}_z+[\frac{eE_l}{m\omega\gamma_o}\sin(kz-\omega t+\theta)+\frac{\omega_{ce}k_o}{\gamma_o\kappa^2}\\ &\cos k_o z]\hat{e}_x+[\frac{eE_l}{m\omega\gamma_o}\cos(kz-\omega t+\theta)\\ &+\frac{\omega_{ce}k_o}{\gamma_o\kappa^2}\sin k_o z]\hat{e}_y.\end{aligned} \tag{4}$$

The ponderomotive force can be calculated as[19]

$$F_z=\frac{e\omega_{ce}E_l}{c\gamma_o}[(1+\frac{\omega_{pe}^2}{\gamma_o\kappa^2c^2})\frac{1}{k}-\frac{k_o}{\kappa^2}]\cos[(k+k_o)$$

$$z-\omega t+\theta)] \tag{5}$$

and the pondromotive potential is

$$\phi(z)=\phi_o \sin[(k+k_o)z-\omega t+\theta] \tag{6}$$

where ϕ_o is the amplitude of the ponderomotive potential and is written as

$$\phi_o=-\frac{e\omega_{ce}E_l}{c\gamma_o(k+k_o)}[(1+\frac{\omega_{pe}^2}{\gamma_o x^2 c^2})\frac{1}{k}-\frac{k_o}{x^2}]. \tag{7}$$

In the cold beam, weak pump, Raman regime, the dominant saturation mechanism appears to be electron trapping in the electrostatic idler wave. However, in the later stage of operation when the EM wave is amplified to some extent, the saturation of the instablility is due to electron trapping by the ponderomotione potential.

Then, we write equation of the motion of an electron as

$$m\gamma_o^3(\frac{\partial}{\partial t}+v_{oz}\frac{\partial}{\partial z})v_z'=-eE_z'+F_z \tag{8}$$

where E_z' is the electrostatic field, F_z is the ponderomotive force and v_z' is the perturbed longitudinal velocity.

The intrinsic efficiency of an FEL with constant wiggler parameters is limited to a few percent. It has been suggested that the efficiency can be enhanced by the adiabatic change of the wiggler parameters so as to gradually slow down the ponderomotive wave and any particle in it. To consider the tapering of the interaction parameters,[20] we rewrite Eq. (8) as

$$m\gamma_o^3\ddot{z}'=-e\frac{\partial}{\partial z'}\Phi(z')+\frac{\partial}{\partial z'}\phi_o\sin[(k+k_o)z'] \\ -m\gamma_o^3\dot{v}_o \tag{9}$$

were $z'+\int^t v_o dt$ is the axial position of a particle, v_o is the velocity of the ponderomotive well, and $\Phi(z')$ is the scalar potential which generated the electrostatic field. The last term on the right in Eq. (9) represents that inertial force due to deceleration with $v_o=\frac{dv_o}{dt}<0$. The potential Φ, which generated the axial electric field, is a combination of the electrostatic potential and the axial vector potential.

The potential Φ satisfies the modified Poission Equation[20]

$$\gamma_o^2\nabla_\perp^2\Phi+\frac{\partial^2\Phi}{\partial z'^2}=-4\pi en. \tag{10}$$

For a broad beam, the potential can be represented by two parts, $\Phi=\bar{\Phi}+\tilde{\Phi}$ where $\bar{\Phi}$ is independent of the axial position $z, \gamma_o^2\nabla_\perp^2\bar{\Phi}=-4\pi e\bar{n}$ where $\bar{n}$ is the average density, and $\tilde{\Phi}$ is periodic in z with a period equal to that of the ponderomotive wave. Then we have

$$\frac{\partial^2\Phi}{\partial z'^2}=-4\pi e(\bar{n}-n). \tag{11}$$

Particles satisfying Eq. (9) have a constant of motion

$$\varepsilon=\frac{1}{2}m\gamma_o^3\dot{z}'+\phi_o\psi(\xi) \tag{12}$$

where $\xi=(k+k_o)z'$ is a normalized distance and $\psi(\xi)$ is a dimensionless effective potential well, $\psi(\xi)=\frac{e\Phi(\xi)}{\phi_o}-\sin\xi-\alpha\xi$, and $\alpha=\frac{m\gamma_o^3|\dot{v}_o|}{(k+k_o)\phi_o}$ measures the deceleration rate. If we adopt the previous normalizalion for length and potential, Eq. (11) yields a second order nonlinear differential Eq. for $\psi(\xi)$,

$$\frac{d^2\psi(\xi)}{d\xi^2}=\sin\xi+\bar{\eta}-\eta(\psi) \tag{13}$$

where $\bar{\eta}=\frac{4\pi e^2\bar{n}}{(k+k_o)\phi_o}$ measures the average density and $\eta(\psi)$ measures the local density. As the particles are slowed down they give their energy to the field.

Balancing the spatial rate of increase of wave energy with lost by paticles one finds

$$c\frac{\partial}{\partial z}(\frac{E_l^2}{8\pi})=-\bar{n}mc^2\frac{d\gamma_o}{dt}=m\bar{n}\gamma_o^3 v_o|\dot{v}_o|. \tag{14}$$

We take the wiggler wavelength to be

$$\lambda_o(z)=\lambda_o[1-\frac{L_t}{L}z] \tag{15}$$

where L_t represents the percentage decrease of the wiggler period, and obtain

$$\frac{dk_o(z)}{dz}=\frac{L_t\cdot 2\pi}{L\lambda_o}, \tag{16}$$

and since the phase velocity of the ponderomotive wave v_o is $\frac{\omega}{k+k_o(z)}$, we write

$$\frac{dv_o}{dk_o}=-\frac{\omega}{(k+k_o)^2}. \tag{17}$$

Then we obtain

$$\frac{dv_o}{dt}=\frac{v_{oz}L_t 2\pi}{L\lambda_o}[-\frac{\omega}{(k+k_o)^2}]. \tag{18}$$

Therefore we get the absolute value of $\dot{v}_o$,

$$|\dot{v}_o| = \frac{v_{oz} L_t 2\pi\omega}{L\lambda_o (k+k_o)^2}. \tag{19}$$

Substitution of $|\dot{v}_o|$ into α and $\bar{\eta}$ yield

$$\alpha = \frac{m\gamma_o^3}{(k+k_o)\phi_o} \cdot \frac{v_{oz} L_t 2\pi\omega}{L\lambda_o (k+k_o)^2}, \tag{20}$$

$$\bar{n} = \frac{\bar{\eta} m \gamma_o^3 v_{oz} L_t \omega}{2e^2 (k+k_o) \alpha L \lambda_o}. \tag{21}$$

We take $\omega = kc = \zeta k_o c$, $\frac{k}{k_o} \equiv \zeta$.

The formula for $\bar{n}$ is given by

$$\bar{n} = \frac{m\gamma_o^3 \bar{\eta} c^2 \sqrt{1-1/\gamma_o^2}\, L_t \zeta}{2e^2 L \lambda_o \alpha\, (\zeta+1)}, \tag{22}$$

and then we can obtain the formula for the gain coefficient

$$g = \frac{\partial}{\partial z} \ln E_l^2 = \frac{2}{E_l} \cdot \frac{\partial E_l}{\partial z}$$

where
$$\frac{\partial E_l}{\partial z} = \frac{4\pi m \bar{n} \gamma_o^3 v_o |\dot{v}_o|}{E_l c}. \tag{23}$$

Using Eqs. (19), (21), (23), the final formula for the gain coefficient can be expressed as

$$g = \frac{2\alpha\bar{\eta}\sqrt{1-\frac{1}{\gamma_o^2}}\,(\zeta+1) k_o \omega_{ce}^2}{c^2 \gamma_o^2} \left[\left(1+\frac{\omega_{pe}^2}{\gamma_o \kappa^2 c^2}\right)\frac{1}{k} - \frac{k_o}{\kappa^2}\right]^2. \tag{24}$$

III. NUMERICAL CALCULATION AND RESULTS

In this section, we investigate the performance of a tapered FEL with guide field. Parameters α and $\bar{\eta}$ are calculated as follows.[20] The boundary condition that is applied to $\psi(\xi)$ in Eq. (13) is that $\psi(\xi)+\alpha\xi$ is periodic in ξ with period 2π. So Eq. (13) was integrated backwards in ξ for different values of $\bar{\eta}$ until one was found for which $\psi'(\xi_o - 2\pi) = 0$, where ξ_o is the location of the local maximum. The corresponding value of α, the deceleration was determined from

$$\alpha = \frac{1}{2\pi}\left[\psi(\xi_o - 2\pi) - \psi(\xi_o)\right].$$

Their values are 0.409 and 0.308, respectively. The gain

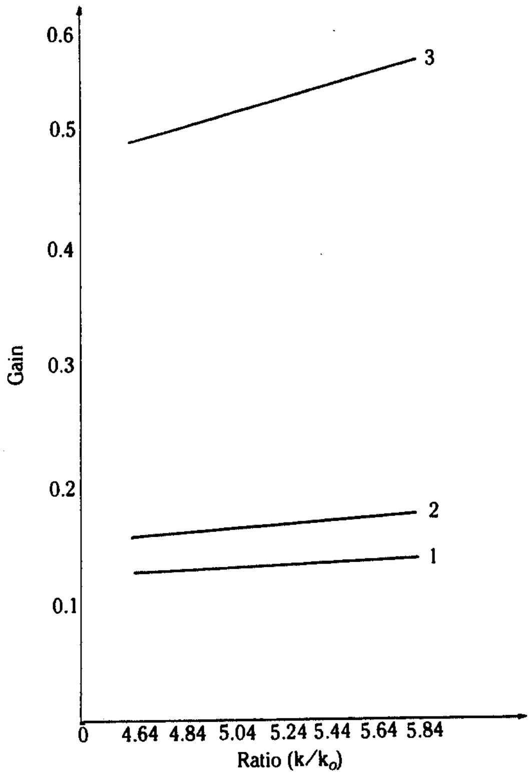

Fig. 1. The gain (coefficient) as a function of wavenumber for beam energy $\gamma_o = 2$. Lines (1), (2) and (3) represent three different regimes of the wiggler and guid magnetic field. Here the wiggler period is 2 mm. (1) $B_{oz} = 21$ KG, $\delta B = 400$ G, (2) $B_{oz} = 30$ KG, $\delta B = 400$ G, (3) $B_{oz} = 21$ KG, $\delta B = 800$ G.

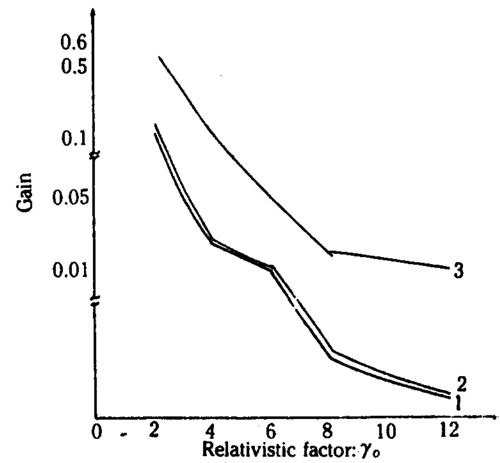

Fig. 2. The gain coefficient for different beam energies from $\gamma_o = 2$ to $\gamma_o = 12$. Here the wiggler period is 2 mm. (1) $B_{oz} = 21$ KG, $\delta B = 400$ G, (2) $B_{oz} = 30$ KG, $\delta B = 400$ G, (3) $B_{oz} = 21$ KG, $\delta B = 800$ G.

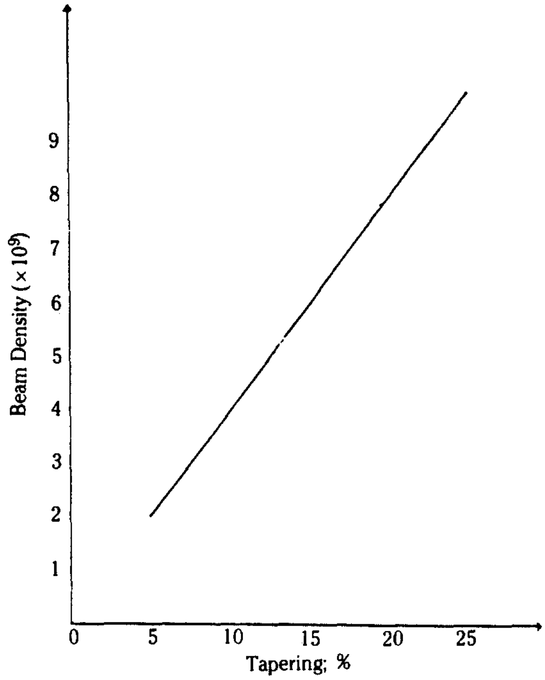

Fig. 3. The optimal beam density as a function of percent decrease in the wiggler period from 5% to 25% for beam energy γ_o=2. Here the wiggler period is 2 mm, and B_{oz}=21 KG, δB=400 G.

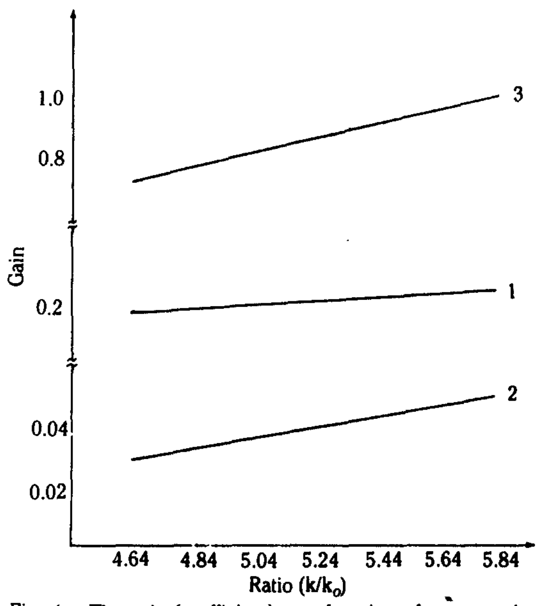

Fig. 4. The gain (coefficient) as a function of wavenumber for beam energy γ_o=2. Lines (1), (2), and (3) represent three different regimes of the wiggler and guide magnetic field. Here the wiggler period is 2 cm. (1) B_{oz}=21 KG, δB=400 G, (2) B_{oz}=30 KG, δB=400 G, (3) B_{oz}=21 KG, δB=800 G.

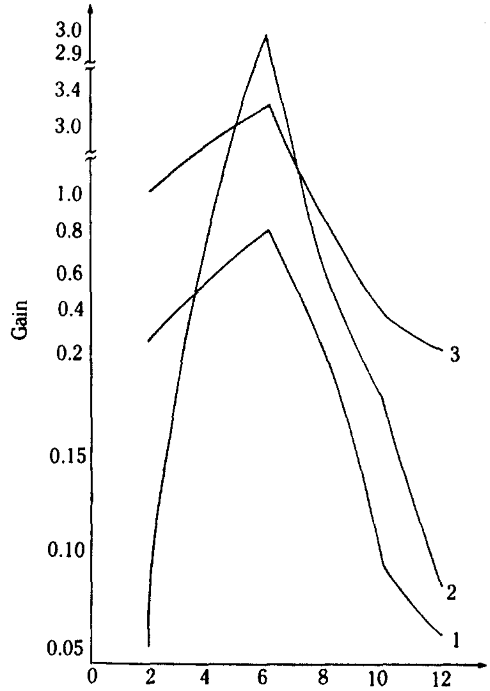

Fig. 5. The gain coefficient for different beam energies from γ_o=2 to γ_o=12. Here the wiggler period is 2 cm. (1) B_{oz}=21 KG, B=400 G, (2) B_{oz}=30 KG, δB=400 G, (3) B_{oz}=21 KG, δB=800 G.

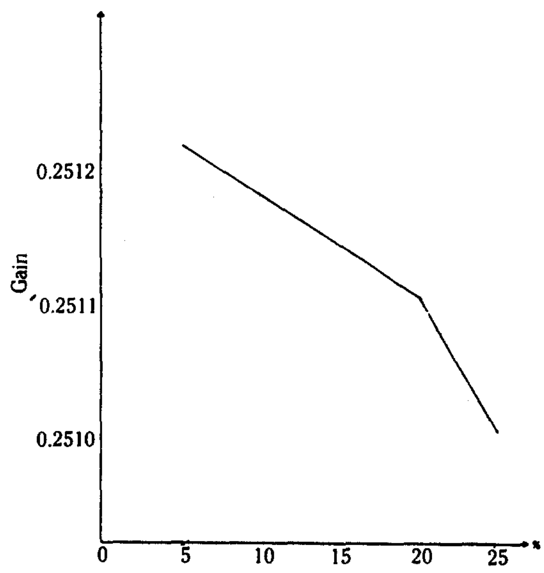

Fig. 6. Gain as a function of percent decrease in the wiggler period from 5% to 25% for beam energy γ_o=2. Here the wiggler period is 2 cm and B_{oz}=21 KG, δB=400 G.

is plotted as a function of wavenumber for three different parameter regimes in Fig. 1. In this case, we chose different values for the wavelength and the wiggler length, values of 2 mm and 1 m, respectively.

First, we consider the case where the guide field is $B_{oz}=21$ KG and the wiggler field $\delta B=400$ G. In this case, the gain ranged from 0.12 to 0.14. Second, when the guide field is increased to some extent, e.g. 30 KG and the wiggler field is the same as before, the gain is slightly greater than the first case. Third, when the guide field $B_{oz}=21$ KG and the wiggler field is doubled, the calculated gain is enhanced by about four times over the first case. In Fig. 2, the gain is plotted as a function of a relativistic factor. In Fig. 3, the optimal beam density is plotted as a function of the degree of tapering in the wiggler period.

Next, we fix the guide field and the wiggler strength as before and choose a different value for the wiggler period, 2 cm, and observe the linear gain relation in Fig. 4 We also note, comparing with Fig. 1, that the gain coefficient for $B_{oz}=21$ KG is higher than that for $B_{oz}=30$ KG, but when the wiggler field strength is doubled, the gain is enhanced about four times. In Fig. 5, as the relativistic factor is increased, the gain increases gradually and reaches its highest valu at $\gamma_o=6$, and afterwards it decreases. In Fig. 6, we can note that as the degree of taper in the wiggler period becomes larger, the gain decreases.

IV. CONCLUSIONS

A tapered free electron laser with a guide field is analyzed. The equation of motion for an electron in this FEL is presented, and a formula for calculating the gain is also presented. Our intent is to find the dependence of the gain on the normalized vector potential, the relativistic factor, the axial guide field, the wiggler field strength, and the tapering wiggler period.

When the wiggler period is 2 mm and the wiggler length is 1 m, the gain increases as the velocity of the electron beam reduces within relativistic limit. Also we can note that it is better to increase the wiggler field than to increase the guide field for gain enhancement. With increase in the degree of taper in the wiggler period, the optimal beam density is increased.

In the case where the wiggler period is 2 cm and the wiggler length 1 m we observe that the gain reaches its highest value at $\gamma_o=6$, and that it is better to increase the guide field than to increase the wiggler period. The gain of the tapered FEL decreases with the degree of taper. The gain depends on beam velocity, wiggler field strength, wiggler period, axial guide magnetic field, and the degree of taper in the wiggler period.

ACKNOWLEDGEMENT

We are grateful to Dr. Jungsik Choi and Dr. G.S. Cho for their helpful comments.

REFERENCES

[1] D. A. G. Deacon, L. R. Elias, J. M. J. Madey, G. J. Ramian, H. A. Schwettman, and T. I. Smith, Phys. Rev. Lett., **38,** 897 (1977).
[2] T. C. Marshall, S. Talmadge, and P. Efthimion, Appl. Phys. Lett., **31,** 320 (1977).
[3] V. L. Granatstein, P. Sprangle, J. Appl. Phys. **46,** 2021 (1975).
[4] Y. Carmel and J. A. Nation, J. Appl. Phys. **44,** 5268 (1973).
[5] T. Kwan and J. M. Dawson, Phys. Fluids **22,** 1089 (1979).
[6] L. Friedland and I. B. Bernstein, Phys. Rev. Lett., **26,** 2778 (1982).
[7] R. W. Warren et al., IEEE J. Quan. Elect. **19,** 391 (1983).
[8] D. W. Feldman et al., IEEE J. Quan. Elect. **23,** 1476 (1983).
[9] C. A. Brau, IEEE J. Quan. Elect. **16,** 335 (1980).
[10] J. M. Slater et al., IEEE J. Quan. Elect. **19,** 374 (1983).
[11] N. M. Kroll et al., IEEE J. Quan. Elect. **17,** 1436 (1981).
[12] W. P. Marable, C. M. Tang, and P. Sprangle, Nuclear Inst. and Meth. **A259,** 210 (1987).
[13] R. A. Freedmann and W. B. Colson, Opt. Comm., **52,** 409 (1985).
[14] H. Boehmer et al., Phys. Rev. Lett. **48,** 141 (1982).
[15] B. E. Newnam et al., IEEE J. Quan. Elect. **21,** 867 (1985).
[16] J. M. Slater et al., Appl. Phys. Lett. **43,** 745 (1983).
[17] K. R. Hartzell Jr., Phys. Lett. **A122,** 476 (1987).
[18] T. Orzechowski et al., Phys. Rev. Lett. **57,** 2172 (1986).
[19] Tae Hun Chung, J. Kor. Phys. Soc. **21,** 322 (1987).
[20] T. M. Antonsen, Jr., Phys. Rev. Lett. **58,** 211 (1987).

Journal of the Korean Physical Society, Vol. 22, No. 3, September, 1989

축방향 유도자기장을 가진 Tapered 자유전자레이저의 이득계산

정태훈·김형진
동아대학교 물리학과

(1989년 3월 23일 받음)

축방향 유도자기장을 가진 tapered 자유전자레이저를 선형유체 모형으로 해석하였다. 전자의 운동방정식, 운동상수 그리고 이득계수를 계산하였고 이득계수의 정규화된 벡터포텐셜, 위글러주기의 감소도, 위글러장과 유도자기장의 세기, 그리고 위글러주기 등에 대한 의존도를 조사하였다.